EGTRIB Journal
JOURNAL OF
THE EGYPTIAN SOCIETY OF TRIBOLOGY
VOLUME 22, No. 3, July 2025, pp. 65 - 79 **ISSN 2090 - 5882**
(Received January 09. 2025, Accepted in final form June 21. 2025) **jest.journals.ekb.eg**

IDENTIFICATION OF SOLID CONTAMINANTS IN LUBRICATING OIL IN CEMENT INDUSTRY

Shimy K. S., Khashaba M. I. and Ali W. Y.

Department of Production Engineering and Mechanical Design, Faculty of Engineering, Minia University, El-Minia, EGYPT.

ABSTRACT

Oil monitoring is a key component of successful condition monitoring programs. It can be used as a predictive tool to identify the wear modes of rubbing parts and diagnose the faults in machinery. By analyzing the oil samples, the residual life of used oil is determined and a fault in the machine can be diagnosed before the machine has to be shut down. Wear debris generated from two moving surfaces inside a machine is a direct wear product of operating machinery. The study of the debris can reveal wear mechanisms, wear modes and wear phases undergoing in the machine.

The aims of this work are to establish an atlas of the solid particles contaminated in the lubricating oils of the machines used in the cement industries. This atlas helps in identifying wear particles and differentiate between them and the solid contaminants from the raw materials in the industry. The raw material used in cement manufacturing that enter to the oil as a contaminant in the oil confuses the wear debris analysis due to the nearest appearance under the microscopic inspection with that generated from wear process. Therefore, the proposed solid contaminants atlas illustrates how to distinguish between particles that came from the raw materials and wear debris while performing the oil analysis. The particles of the raw materials are collected and inspected by optical microscopic. Besides, solid contaminants are collected from the oil filters of two main equipment used in cement industry and washed with suitable solvent, then filtrated by membrane filter.

The results revealed that the difference between clinker particles and wear debris can be achieved by inspection of the sample using cross-reflected light microscope. The fatty clay particles appear in brown color, while Fe_2O_3 particles appear in a dark brown or light black color. Limestone particle appears as crystals. The air cooled slag particles appear in light brown color containing small dark brown areas due to the low content of Fe_2O_3. Finally, water cold slag appears as glass particles.

KEYWORDS

Wear debris, condition monitoring, oil analysis, wear particles atlas, cement industry.

INTRODUCTION

The wear of machine elements is the main cause of their failure. Monitoring of wear clears the operational condition of machines, [1 - 6]. The lubricating the machines reduces the friction. Wear particles contaminating the oil have specific information about the degradation and failure of the system. Wear particles give early diagnosis of machine failure and facilitate the decision-making to achieve maintenance. The common methods of monitoring wear particles are the spectrometer that monitors particles smaller than 10 µm in size and the magnetic plugs for larger particles than 1000 µm. For particles larger than 10 µm, wear particle analysis can reveal the causes of failure. The online wear particle analysis is necessary to detect mechanical failures and avoid sudden failures. An optical direct imaging method was developed using high precision particle analyzer in online acquisition of particle images contaminating the circulating oil system to identify some types of wear particles, such as normal, sliding, fatigue, cutting, sphere, and fiber, using their images, [7 – 12]. Condition monitoring of the internal combustion engines is essential, where the cylinder liner ensurs the perfect combustion of the gas preventing from leakage. The cylinder liner is suffering from several factors that influence its wear rate, so that the engine performance and failure can be expected. Therefore, wear of the cylinder liner should be monitored, [13 – 18], to control the engine performance.

Oil analysis is the major technique of machine condition monitoring in predictive maintenance, [18 - 30]. A Ferrographic oil analysis for samples of oil in fluid power control system is achieved, where shape and size of contaminant are defined. The cleanliness level of oils is based can be determined by oil analysis. Enhancing the efficiency of filtration is recommended for oil cleanliness. The critical cause of wear is the solid contaminants in the oil. Their sources may be from the dirt enters the system during assembly and reassembly, environment and wear debris generated inside the system. Fresh oil can contain sand particles and polymeric fibers generated form the degradation of fillers and seals. based on that observation, it is necessary that the cleanliness of base oil and lubricant additives must be controlled during production. Contaminants particles are divided in according to their size, quantity, morphology and composition. Besides, their concentration indicates the severity and rate of wear. Oil analysis supplies specific information about the condition of the of the machine elements. The composition of particles is determined by the Ferrogram that can reveal their origin, by the aid of their color. When the Ferrogram is heated up to 330°C for 90 seconds, the blue color indicates low alloy steel, while straw color indicates cast iron.

The present work establishes a solid particles atlas for cement industry to determine and distinguish between the contaminant particles. The main materials used in cement manufacturing are lime stone, clay, slag, iron ore and clinker.

EXPERIMENTAL

Oil samples were collected from the oil filters; the filtration unit of the raw mill and cement mill. Then the filter material was removed from the filter housing. Square piece of 20 × 20 mm from the pleated papers was cut then ultrasonically scrubbed in

50 ml of normal heptane in order to redisperse the particles for 45 minutes. Then the wash was filtered by 0.4 μm paper membrane. The solid particles deposited on the membrane were considered as the wear and solid contaminants as well as oxidation products. The membrane was washed by 50 ml of benzol to dissolve the oxidation products. Carl Zeiss microscope supported by the reflected and transmitted lights as well as digital camera for photographing. Inspection of the membrane by the microscope displayed the types of contaminants and wear particles. The ferrous particles were separated from the filtrates by magnetic rod covered by a plastic sheet to ease the removal of the attracted ferrous particles.

RESULTS AND DISCUSSION

The main components for the clinker and their percentage are shown in Table 1, [31].

Table 1 Clinker chemical composition

SiO_2	Al_2O_3	Fe_2O_3	CaO
20 – 23 %	4 – 6%	4 – 6 %	50 – 66 %

The above-mentioned components integrate to produce the clinker from C_3S, C_2S, C_3A, C_4AF and CaO.

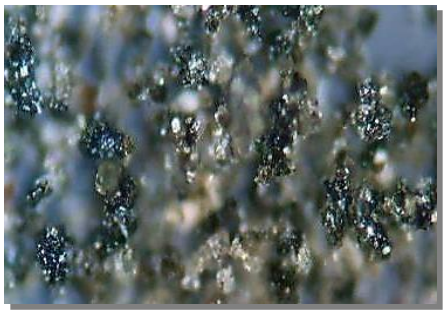

Fig. 1 Accumulated clinkers particles appear under cross-reflected light, magnification ×50.

Accumulated Clinkers particles appear under cross-reflected light microscopic inspection with magnification ×50 as a black particle character with small bright particles due to the presence of silica in its constituents are shown in Fig. 1. The inspection for accumulated particles shall be of small magnification because the sample is not polished which affect the contrast. Figure 2 shows clinker particle under transparent light microscopic inspection with magnification ×50 appears as black particles because it did not transmit the light. Clinker appears under transparent light microscopic inspection as black of small bright particles due to silica components in the clinker. Clinker particle under cross-transparent light microscopic inspection with magnification ×200 appear as stone particles in black or dark blue color, Fig. 3. Clinker particles under the cross-reflected light microscopic inspection with magnification ×100 appear in clinker phases shape and the CaO components appear clear, Fig. 4.

Fig. 2 Clinker particle under transparent light, magnification ×50.

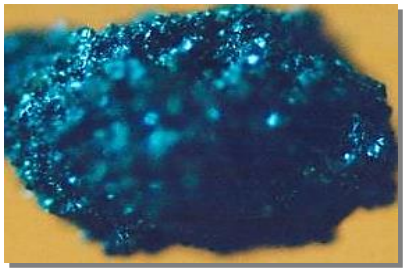

Fig. 3 Clinker particle under cross-transparent light, magnification ×200.

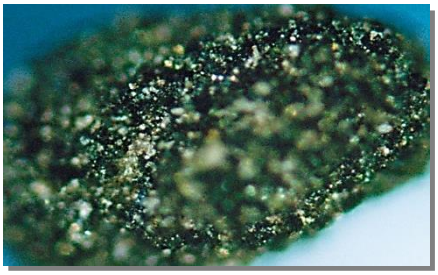

Fig. 4 Clinker particle under the cross-reflected light, magnification ×100.

Clay consists of hydrated silicates of aluminum. Clay used in cement industry as a source for silica and alumina in cement product. The main components of clay are SiO_2, Al_2O_3, Fe_2O_3, MgO and CaO. Clay has two types, fatty and sandy clay. Fatty clay has silica percentage not more than 60% and 10% ferrous oxide (Fe_2O_3). The main components for the fatty clay and their percentages are shown in Table 2.

Table 2 Fatty clay chemical composition

SiO_2	Al_2O_3	Fe_2O_3	CaO
48 – 60 %	10 – 16 %	5 – 10 %	3 – 8 %

Fatty clay particles under inspection of cross reflected light microscope with magnification ×50 appear as light brown color husks particle character with small darky brown color areas due to the Fe_2O_3 contained in its components, Fig. 5.

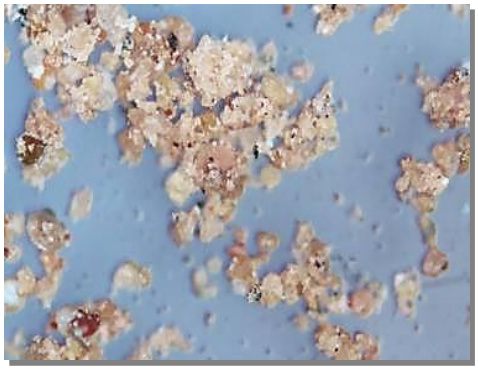

Fig. 5 Accumulated fatty clay particles under cross-reflected light, magnification ×50.

Fatty clay particles under reflected light microscopic inspection with magnification ×50 gives clear appearance for the dark brown area, which indicates Fe_2O_3 components, Fig. 6. Fatty clay particle under transparent light microscopic inspection with magnification ×50 the light penetrates though the silica components, the area have high content of Fe_2O_3 is still in low brightness than the light brown area that contains high content of silica, Fig. 7. Fatty clay particles under reflected light microscopic inspection with magnification ×100 appear in bright red color and the silica component do not appear, Fig. 8.

Fig. 6 Fatty clay particles under reflected light, magnification ×50.

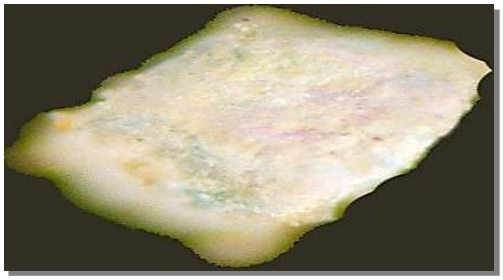

Fig. 7 Fatty clay particle under transparent light, magnification ×50.

Fig. 8 Fatty clay particles under reflected light, magnification ×100.

Sandy clay has silica content up to 60 % and the content of Fe_2O_3 is 5 % that leads to less of appearance of Fe_2O_3 in the particles under microscopic inspection. The main components for the sandy clay and their percentages are shown in Table 3.

Table 3 Sandy clay chemical composition

SiO_2	Al_2O_3	Fe_2O_3	CaO
> 60 %	8 %	5 %	4 %

The photomicrograph of sandy clay particles under cross-reflected light microscopic inspection with magnification ×100 that appear as crystal husks particles is shown in Fig. 9. Sandy clay particle under the cross-reflected microscopic light inspection with magnification ×100 shows the dark brown areas that indicates Fe_2O_3.

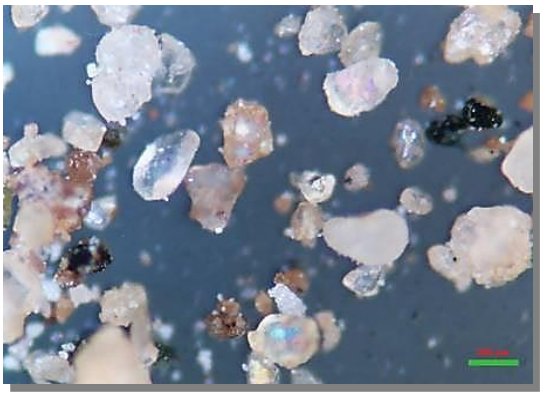

Fig. 9 Accumulated sandy clay particles under cross-reflected light, magnification ×50.

Fig. 10 Sandy clay particle under cross-reflected light, magnification ×100.

Iron ore used in cement industry to adjust the ferrous ratio in cement. Most of the components of iron ore is Fe_2O_3 up to 90%. Due to this content, iron ore during oil analysis looks like the iron oxide generated by corrosive wear. The main components of the iron ore and their percentages are shown in Table 4.

Table 4 Iron ore chemical composition

SiO_2	Al_2O_3	Fe_2O_3	CaO
2 – 5 %	1.5 %	60 - 90 %	2 %

Figure 11 shows iron ore particles under transparent light microscopic inspection with magnification ×50 appear as black particles due to high content of Fe_2O_3 that did not transmit the light. Iron ore particles under cross-transparent light microscopic inspection with magnification ×50 appear as black particles due to high Fe_2O_3 content that did not transmit the light but the small content of silica reflects the light and appears as small bright points. This is the first indication to differentiate between the iron ore contaminants and the corrosive wear particles, Fig. 12. Iron ore particles under cross-reflected light microscopic inspection with magnification ×50 appear as red particles including small bright silica particles, Fig. 13.

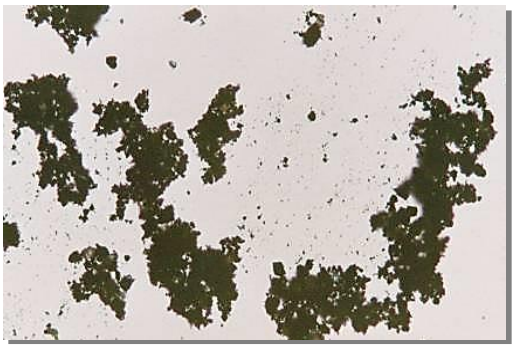

Fig. 11 Accumulated iron ore particles under transparent light magnification X50.

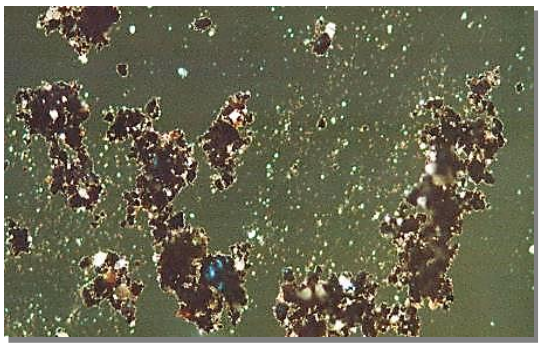

Fig. 12 Accumulated iron ore particles under cross-transparent light, magnification X50.

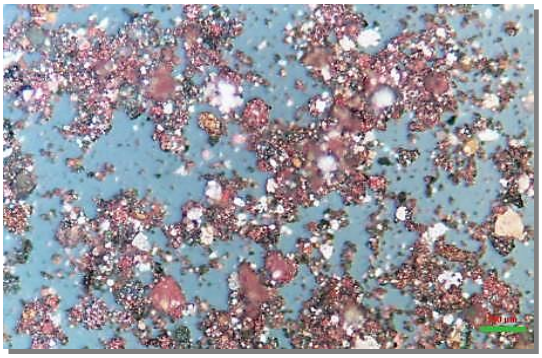

Fig. 13 Accumulated iron ore particles under cross-reflected light, magnification ×50.

Iron ore particle under reflected light microscopic inspection with magnification X100 appears as light red particles and sometimes contains little bright points due to small percentage form silica in its components, Fig. 14.

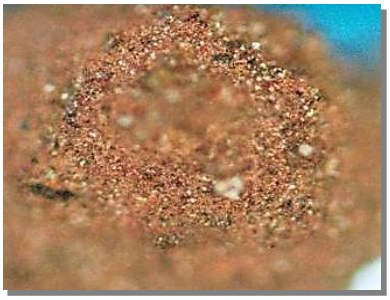

Fig. 14 Iron ore particle under reflected light, magnification X100.

Limestone is one of the main components in cement manufacturing, Fig. 15. The main components for lime stone is $CaCo_3$ of percentage is ranging between 75 to 98%. Limestone enters the oil when it attacks the equipment as contaminant and be in the form of sludge in the button of the gearbox or in oil filter. Limestone appears accumulated due to the content for CO_2 in its components, which generates bond

between the particles. Figure 15 shows limestone under transparent light with magnification ×50 as crystals due to its transmittance of the light through the particles. It is white in color that makes it easy to be distinguished during oil analysis after diluting or washing the sample with solvent to dissolve the oil.

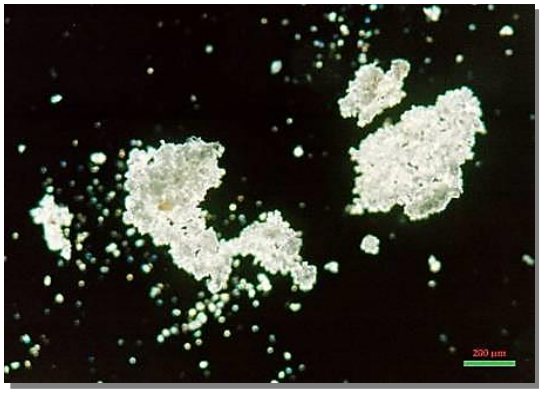

Fig. 15 Limestone accumulated particles under cross-reflected light with magnification ×50.

Slag is used in cement industry to adjust the cement components ratio during mix design and add ready calcite material to the process to add heat value or in other words reduce the fuel consumption during the process. The main components of slag are SiO_2, Al_2O_3, Fe_2O_3, and CaO. Slag is divided into two categories namely air cooled slag that includes air cooled slag high ferric and air cooled slag low ferric. The difference between the above mentioned types is the ferrous oxide percentage in its components. The second type is water cooled slag that is cooled with water after extraction from the iron furnace. Air cooled slag high ferric as mentioned before is cooled naturally with air after extraction from the iron furnace. The main components for the air-cooled slag high ferric and their percentages are shown in Table 5.

Table 5 Air cooled slag high ferric chemical composition

SiO_2	Al_2O_3	Fe_2O_3	CaO
35 %	18 %	25 - 30 %	5 %

High air cooled slag particles under cross reflected light microscopic inspection with magnification ×50 have the same appearance as the fatty clay particles. The only difference is that the dark brown areas increased due to the increase of Fe_2O_3 ratio from mostly 10% in fatty clay to 25 – 35% in air cooled slag, Figs. 16, 17.

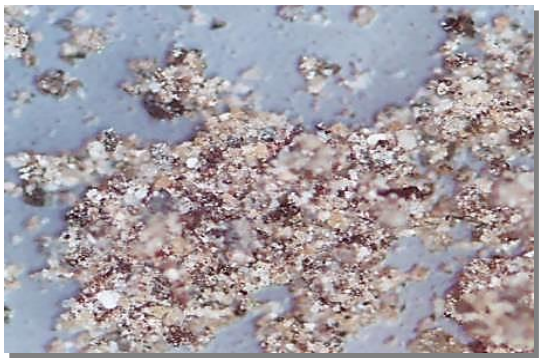

Fig. 16 Air cooled slag particles under cross reflected light, magnification ×50.

Fig. 17 Air cold slag under reflected light, magnification ×50.

Air cold slag high ferric under reflected light microscopic inspection with magnification ×50 appears as red particles, which makes conflict with the appearance of iron ore particles under this type of inspection. However, the difference is that the iron ore particle contains lower percentage of silica (2 – 5%) than the air cold high ferric slag 35% that get a more bright areas in the particle, Fig. 3.40.

Air-cooled slag low ferric as mentioned before is cooled naturally with air after extraction from the iron furnace. The main components for the air-cooled slag and their percentages are shown in Table 6.

Table 6 Air cooled slag chemical composition.

SiO_2	Al_2O_3	Fe_2O_3	CaO
38%	20 %	5 - 10 %	5 %

Accumulated air cooled slag low ferric particles under cross reflected light microscopic inspection with magnification ×50 appear as white husks with dark brown or black areas due to ferrous oxide components percentage which is lesser than air cold slag high ferric, Fig. 18.

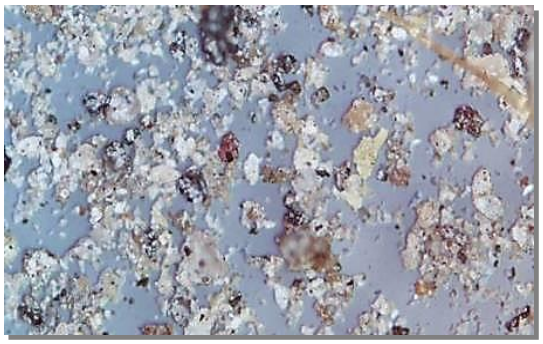

Fig. 18 Air cooled slag low ferric particle under cross reflected light, magnification ×50.

Air cooled slag low ferric under cross transparent light microscopic inspection with magnification ×50 appear as lighted particles due to low ferrous oxide percentage and high silica percentage as compared with air cooled slag high ferric, Fig. 19.

Fig. 19 Air cooled slag low ferric under cross transparent light, magnification ×50.

Air cooled slag low ferric under reflected light microscopic inspection with magnification ×50 appear in light brown color containing small areas of dark brown due to less percentage of ferrous oxide components. Figure 3.48 shows air-cooled slag under cross-reflected light microscopic inspection with magnification ×50. The small percentage from ferrous oxide components is clearly shown. it can be a judge to identify this type of oil contaminants.

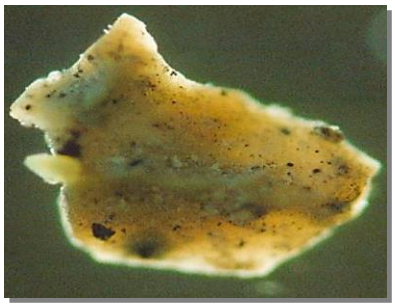

Fig. 20 Air cooled slag under cross reflected light, magnification ×50.

Water cooled slag as mentioned before is cooled by water after extraction from the iron furnace. The main components for the water-cooled slag and their percentages are shown in Table 7.

Table 7 Water cold slag chemical composition.

SiO_2	Al_2O_3	Fe_2O_3	CaO
40%	15 %	12 %	5 %

Water cooled slag particles under cross reflected light microscopic inspection with magnification ×50 appears as a glasses in brown color because the cooling process by water transfers its structure to glass phase, Fig. 21.

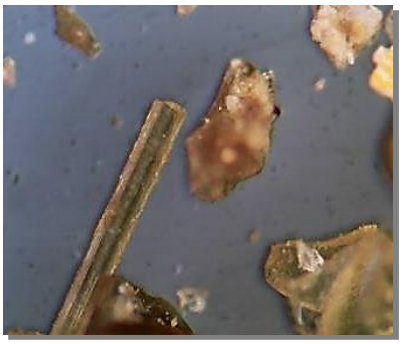

Fig. 21 Accumulated water cooled slag particles under cross reflected light, magnification ×50.

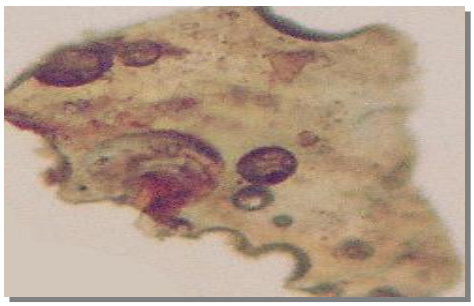

Fig. 22 Water cooled slag under reflected light, magnification ×50.

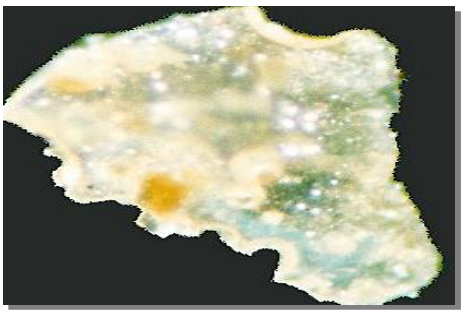

Fig. 23 Water cooled slag under cross reflected light, magnification ×50.

Water cooled slag particles under reflected light microscopic inspection with magnification ×50 appear clear as a particle with light brown color contains small areas of dark brown color due to the little ferrous oxide ratio in its components, Fig. 22. The same particles of water cooled slag under cross reflected light microscopic inspection with magnification X50 appear as glass particles in bright lighted color containing areas with less brightness or lighting due to ferrous oxide components, Fig. 23.

CONCLUSIONS

1. The way to distinguish particles entered the system as contaminants from process material and that generated from wear during the wear debris analysis is to use a cross light with high magnification.
2. Most of the raw materials used in cement manufacturing have a high silica percentage that cause high wear rate.
3. The oil filters used in the equipment have mesh size of 50 µm, which lead to a big size of contaminants in the oil. In addition, use of small mesh oil filter may cause fast oil filter blockage. It is proposed to apply external filtration unit with small mesh filter to keep the system clean.
5. The difference between the clinker particles and the wear debris can be conducted by inspection of the sample using cross-reflected light, where the clinker particles can be shown clearly.
6. The fatty clay particles appear under cross reflected light in its real color towards the brown, while Fe_2O_3 particles appear in a dark brown or light black color. Sandy clay particles appear under cross-reflected light in the real color for clay.
7. Limestone particle appears under transparent light as crystals due to the penetration of the light through the particles.
8. The air cooled slag low ferric particles appear under cross reflected light in light brown color containing small areas from dark brown due to less percentage from ferrous oxide components. Water cold slag appears under cross reflected light as glass particles in bright lighted color containing areas with less brightness or lighting due to ferrous oxide components.

REFERENCES

1. Liu Z., Liu Y., Bai F., Zuo H., Fei H., Dhupia J., "An oil wear particle identification method based on Wasserstein generative adversarial network and improved CNN using a custom-built optical imaging sensor", Measurement 232, 114663, (2024).
2. Lu P., Powrie H. E., Wood R. J. K., Harvey T. J., Harris N. R., "Early wear detection and its significance for condition monitoring, Tribol. Int. 159, 106946, (2021).
3. Hong W., Cai W., Wang S., Tomovic M. M., "Mechanical wear debris feature, detection, and diagnosis: a review, Chin. J. Aeronaut. 31 (5) pp. 867 - 882, (2018).
4. Jia R., Wang L., Zheng C., Chen T., "Online Wear Particle detection sensors for Wear monitoring of mechanical equipment—A review", IEEE Sens. J. 22 (4), pp. 2930 - 2947, (2022).
5. Cao W., et al., "Image denoising and feature Extraction of Wear debris for online monitoring of Planetary Gearboxes", IEEE Access 9, pp. 168937 - 168952, (2021).

6. Yuan Z., Feng S., Tan J., Liu H., "A passive ferro-Particle sensor of lube-oil based on single permanent magnetic ring", IEEE Sens. J. 22 (9) pp. 8565 - 8573, (2022).
7. Liu Z., Zuo H., Bai F., Liu Y., Dhupia J., Jiusi J., Chen Z., "Intelligent classification of online wear particle in lubricating oil using optical direct imaging method and convolutional neural network for rotating machinery", Tribology International 189, 109015, (2023).
8. Jia R., Wang L., Zheng C., Chen T., "Online Wear particle detection sensors for wear monitoring of mechanical equipment - a review", IEEE Sens J, 22 (4), pp. 2930 – 2947, (2022).
9. Lu P., Powrie H. E., Wood R. J. K., Harvey T. J., Harris N. R., "Early wear detection and its significance for condition monitoring", Tribol Int, 159, 106946, (2021).
10. Zhu X., Zhong C., Zhe J., "Lubricating oil conditioning sensors for online machine health monitoring – a review. Tribol Int, 109, pp. 473 - 484, (2017).
11. Hong W., Cai W., Wang S., Tomovic M. M., "Mechanical wear debris feature, detection, and diagnosis: a review", Chin J Aeronaut, 31 (5), pp. 867 - 82, (2018).
12. Peng Y. Cai J., Wu T., Cao G., Kwok N., Peng Z., "WP-DRnet: A novel wear particle detection and recognition network for automatic ferrograph image analysis", Tribol Int, 151, 106379, (2020).
13. Kang J., Shu C., Yang H., Liu Y., Yan C., Zhang F., "Wear prediction of internal combustion engine cylinder liners based on adaptive generative adversarial networks", Results in Engineering, 105740, (2025).
14. Dziubak T., Dziubak S. D., "A study on the effect of inlet air pollution on the engine component wear and operation", Energies, 15 (3), 1182, (2022).
15. Richardson D. E., "Review of power cylinder friction for diesel engines", Journal of Engineering for Gas Turbines and Power, 122 (4), pp. 506 - 519, (2000).
16. Rao X., Sheng C., Guo Z., et al., "A review of online condition monitoring and maintenance strategy for cylinder liner-piston rings of diesel engines", Mechanical Systems and Signal Processing, 165, 108385, (2022).
17. Guo Z. W., Yuan C. Q., Bai X. Q., et al., "Experimental study on wear performance and oil film characteristics of surface textured cylinder liner in marine diesel engine", Chinese Journal of Mechanical Engineering, 31 (1), 52, (2018).
18. Kamiński W., Pożoga I. M., "Possibility of Marine Low-Speed Engine Piston Ring Wear Prediction during Real Operational Conditions", Energies, 16 (3), 1433, (2023).
19. Ali W., and Balog M., "Worn Surface Temperature of the Internal Combustion Engine Determined by the Temper Colours of Wear Particles", the International Conference of Bus Safety, (33. Autóbusz Szakértöi Tanácskozás, Nemzetközi Gepjármü-biztonsági Konferencia), Keszthely, 2002. Szeptember 2 – 4, Hungary, (2002).
20. Ali W., Balogh I. and Balog M., "Wear Particles Generated During Starved Lubricated Sliding of Internal Combustion Engines", Proceedings of INTERFACES' 2002, September 19 – 21, Budapest, (2002).
21. Youssef, M. M., Mahmoud, M. M. and Ali, W. Y., "Detection of Engine Wear by Examining Oil Filter", 7th National Conference of Theoretical and Applied Mechanics, Academy of Scientific Research and Technology, 11 – 12 March, (2003).

22. El-Sherbiny, M. G. and Ali, W. Y., "Ferrographic Oil Analysis OF Wear Particles", Journal of the Egyptian Society of Tribology, Vol. 1, No. 2, July, (2003).
23. Mahmoud, M. M., Hakim, K. A. and Ali, W. Y., "Generation of Wear Particles Before Failure of Internal Combustion Engines", 8th International Conference on Tribology, June 2004, Veszprém, Hungary, (2004).
24. El-Sherbiny, M. G. and Ali, W. Y., "Monitoring Wear of Engines by Examining Wear Particles Retained by the Oil Filter", Journal of the Egyptian Society of Tribology, Vol. 6, No. 2, April 2009, pp. 1 – 12, (2009).
25. El-Sherbiny M. G. and Ali W. Y., "Abrasive Wear of Internal Combustion Engines", Journal of the Egyptian Society of Tribology, Vol. 7, No. 1, January 2010, pp. 1 – 12, (2010).
26. El Sheikh A., Khashaba M. I., Ali W. Y., "Reducing the Mechanical Wear in a Dusty Environment (Cement Factory)", International Journal of Engineering & Technology IJET-IJENS Vol: 11 No: 06, pp. 166 – 172, (2011).
27. Ali W. Y., Youssef M. M., Elhabib O. A., "Auxiliary Filtration of Automotive Engines: Fibrous Depth and Magnetic Filters", The 26th Meeting of Saudi Biological Society, "Climatic Change and Biodiversity", Taif University, Taif, 10 – 12 May, (2011).
28. Elhabib O. A. and Ali W. Y., "Inspection of Wear Particles Retained by the Oil Filters of Automotive Engines", Journal of the Egyptian Society of Tribology Vol. 8, No. 3, July 2011, pp. 15 – 27, (2011).
29. El-Sherbiny, M. G., Mohamed M. K. and Ali, W. Y., "Characterization of Solid Particles Contaminating Automotive Oils by Ferrographic Examination", Journal of the Egyptian Society of Tribology Vol. 9, No. 1, January 2012, pp. 1 – 11, (2012).
30. El-Sherbiny M. G. and Ali W. Y., " Temper Colours of Wear Particles", Journal of the Egyptian Society of Tribology, Vol. 10, No. 3, July 2013, pp. 41 – 50, (2013).
31. Lea's, chemistry of cement and concrete, fourth edition, edited by Peter C. H., (2004).